USCEE 406

UNIVERSITY OF SOUTHERN CALIFORNIA

THE EFFECT OF TIMING ERRORS IN OPTICAL DIGITAL SYSTEMS

R. Gagliardi

Interim Technical Report
August 1971

Department of Electrical Engineering
University of Southern California
Los Angeles, California 90007

ELECTRONIC SCIENCES LABORATORY

USC Engineering

August 1971 USCEE Report 406

Interim Technical Report

The Effect of Timing Errors in Optical Digital Systems

R. Gagliardi

Department of Electrical Engineering

University of Southern California

Los Angeles, California 90007

This work was sponsored by the National Aeronautics and Space Administration, under NASA Contract NGR-05-018-104. This grant was part of the research program at NASA's Goddard Space Flight Center, Greenbelt, Maryland.

This document represents a technical report of a NASA Research Program to study synchronization techniques for optical communication systems. The work is being carried out at the Electrical Engineering Department at the University of Southern California, under NASA Contract No. NGR-05-018-104, with Professor R.M. Gagliardi as principal investigator. This grant is part of the research program being conducted through NASA's Goddard Space Flight Center, Greenbelt, Maryland.

ABSTRACT

The use of digital transmission with narrow light pulses appears attractive for data communications, but carries with it a stringent requirement on system bit timing. In this paper we investigate the effects of imperfect timing in direct detection (non-coherent) optical binary systems using both PPM and on-off keying for bit transmission. Particular emphasis is placed on specification of timing accuracy, and an examination of system degradation when this accuracy is not attained. Bit error probabilities are shown as a function of timing errors, from which average error probabilities can be computed for specific synchronization methods. Of significant importance is the presence of a residual, or irreducible error probability in both systems, due entirely to the timing system, that cannot be overcome by the data channel.

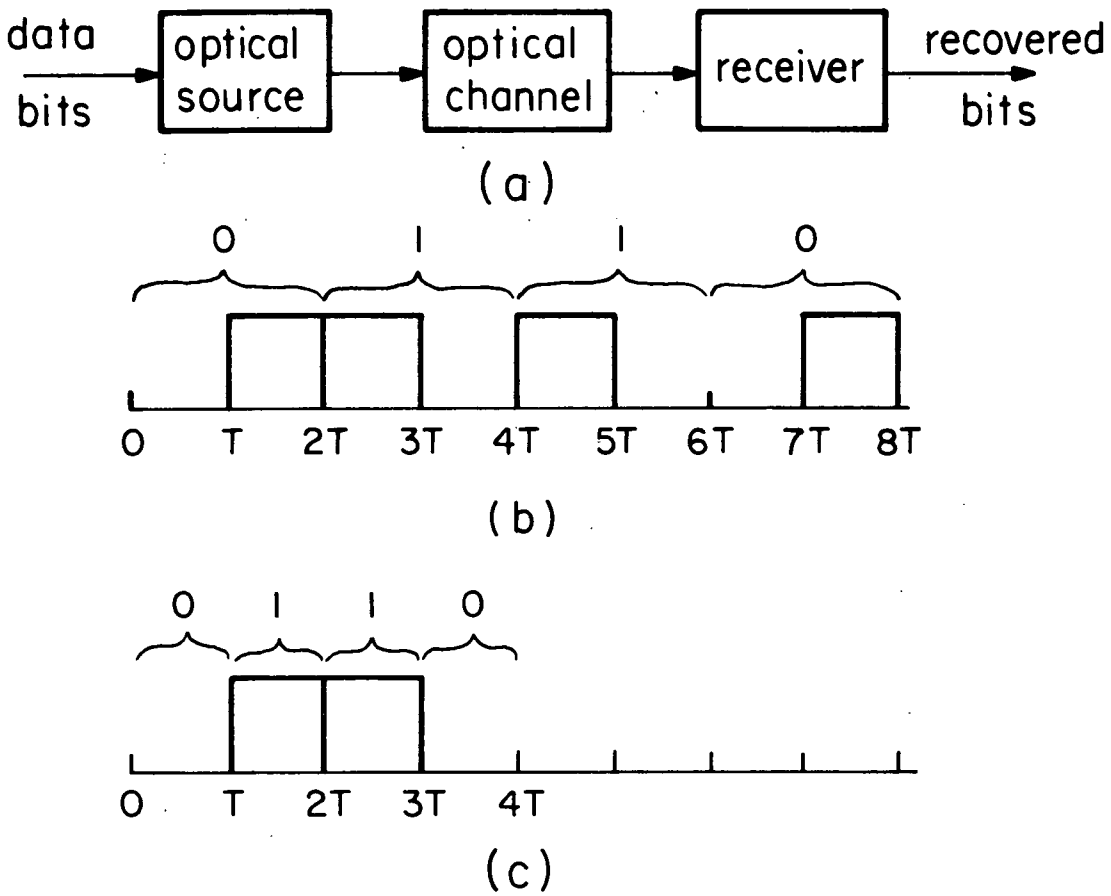
data
bits
optical source
optical channel
receiver
recovered
bits
(a)
0
1
1
0
0 T 2T 3T 4T 5T 6T 7T 8T
(b)
0 1 1 0
0 T 2T 3T 4T
(c)

Figure 1.

Introduction

The ability to generate extremely narrow, high energy light pulses from a laser source has made the optical transmission of digital data extremely attractive for modern communications. This possibility has fostered an exhaustive exploration of optical communication systems, from both a theoretical and hardware point of view (e.g., see [1]). The use of digital transmission with narrow pulses, however, carries with it an extremely stringent requirement on system bit timing--i.e., time control of the system sampling and integration intervals during each data bit. For the most part past analytical studies have assumed perfect system timing, and the degradation caused by timing errors in optical systems have been virtually ignored. In this paper, we investigate the effects of imperfect timing in a direct-detection (non-coherent) optical communication system, with particular emphasis on the specification of timing accuracy, and an examination of the system degradation when this accuracy is not attained.

Consider a general optical digital system as shown in Figure 1a. The system sends bits of information by transmitting bursts of optical energy. One of two possible methods are usually used for encoding the bits. In one the system operates by transmitting a burst of energy in one of two T sec adjacent time intervals to encode a binary bit. This represents a two level pulse position modulated (PPM) mode of transmission and is known to be optimal under various criterion, when constrained in average transmitter power [2]. Thus, for example, the binary sequence 0110

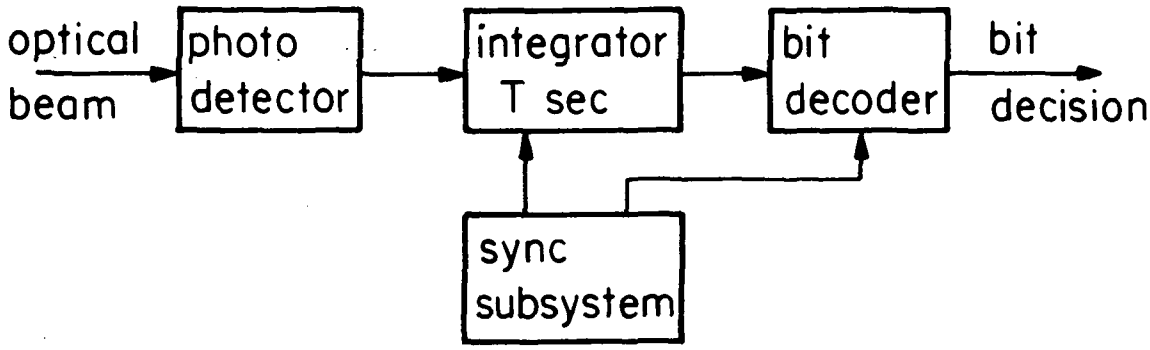
optical
beam
photo
detector
integrator
T sec
bit
decoder
bit
decision
sync
subsystem

Figure 2.

would be transmitted by the optical waveform shown in Figure 1b, where the pulse represents a burst of optical laser energy. We have considered an energy pulse in the first interval to represent a binary one, and an energy pulse in the second interval to represent a binary zero. A second procedure is to use on-off keying, in which the transmitter uses an energy burst for a one, and transmits no energy for a zero. Thus, the waveform 0110 would be transmitted by the energy waveform in Figure 1c. Note that if T is the energy pulse width, then in PPM 2T is the bit interval and information is being transmitted at a rate 1/2T bits/sec, while in on-off keying T is the bit interval and the rate is 1/T bits/sec.

The digital receiver for the system is shown in Figure 2. We shall assume the transmitter and receiver operate diffraction-limited, so that the transmitted energy corresponds to optical energy in a single spatial mode of the optical beam. The received optical beam is photo-detected, and its output is integrated over a T sec interval. The start-stop timing for this integration is provided by a synchronizing subsystem. In PPM, the bit decoder makes a comparison of the integrator output after the first T sec interval of each bit period with that after the second T sec interval, deciding a one or zero accordingly. In on-off keying a threshold test is made at the end of each bit time T, the bit decision depending upon whether the threshold is exceeded or not. The latter system requires accurate knowledge of the expected signal and noise energies in order to properly

set the threshold, representing a serious disadvantage to on-off operation.

If the output of the photo-detector is modeled [3] as a wideband shot noise process (detector bandwidth >> 1/T), then the integrator output after T sec of integration, beginning at time t, is proportional to the shot noise counting process $\underline{k}(t, t+T)$, where

$$\underline{k}(t_1, t_2) = \text{number of photo electrons in } (t_1, t_2) \tag{1}$$

In stating that the integrator value is proportional to (1), we have neglected additive circuit thermal noise which implies the use of high gain, ideal photomultipliers in the photodetection operation. The counting process $\underline{k}(\cdot, \cdot)$ of the photo-detector shot noise is a random point process over the non-negative integers. For the reception of an optical field over (0, T), with the signal energy E and additive, white Gaussian background noise of bandwidth B_0, the probability that the count value $\underline{k}(0, T)$ equals integer k is known to be [4]

$$\text{Prob}[\underline{k}(0, T) = k] \triangleq P_L(k; S, N, D) \tag{2}$$

$$= \frac{(S)^k}{(1+N_0)^{D+k+1}} \exp\left[-\frac{S}{1+N_0}\right] L_k^D\left(-\frac{S}{(1+N_0)N_0}\right)$$

where $S = GE/hf$ = average signal count over (0, T), $N_0 = G[\exp(hf/kT_e - 1)]^{-1}$ = average noise count per mode due to background at temp T_e, h = Planck's constant, f = laser frequency, $D = 2B_0T$, G = photomultiplier gain, and $L_k^D(x)$ is the Laguerre polynomial in x of order D and index k:

$$L_k^D(x) = \sum_{i=0}^{k} \binom{k+D}{k-i} \frac{(-x)^i}{i} \tag{3}$$

The parameter D is the count dimension, or time-bandwidth product. Physically, D+1 is the number of temporal modes observed during the T sec counting interval. The density $P_L(k;S,N,D)$ is called a Laguerre counting density, and is exact for D = 0 and D >> 1, but is only approximate for $D \approx 1$. (This is due to the fact that (2) requires equal eigenvalues in the expansion of the energy function, which is only approximately true for low values of D.) The received average signal energy E over the time interval T can also be written as $E = Q_s T$, where Q_s is the received average power. We then have, alternatively,

$$S = \left(\frac{GQ_s}{hf}\right) T = \mu_s T \tag{4}$$

where μ_s is the average counts per sec (count rate) due to the signal.

Under typical operating conditions, we generally have $N_0 << 1$ and D >> 1, and (2) asymptotically approaches the poisson density [4]

$$\text{Prob}[\underline{k}(0,T) = k] \triangleq P_p(k;S+N)$$

$$\equiv \frac{(S+N)^k}{k!} \exp[-(S+N)] \tag{5}$$

where $N = DN_0$ represents the total noise count in all modes. (For visible wavelengths, N_0 is generally on the order of 10^{-7} - 10^{-6} counts/mode. An optical system at 10 microns operating with a one angstrom optical filter and $T = 10^{-6}$ sec, will generate a D of about 400.) Note that with the poisson assumption, the count probability depends only upon the sum of the signal

and noise count. That is, the count statistics do not distinguish between the effect of signal energy or noise energy, but is determined solely by their cumulative energy.

Error Probabilities

If we transmit a binary PPM signal with fixed signal energy in the signalling interval, then the probability of making a bit error is simply the probability that the count in the non-signalling interval exceeds or equals that of the signalling interval. (If the counts are equal, an equal likely random choice is made concerning that particular bit.) If we denote k_i as the count in the i^{th} interval, $i = 1, 2$, of a bit, then the average error probability is

$$PE = \tfrac{1}{2}\text{Prob}[k_2 > k_1 \,|\text{one sent}] + \tfrac{1}{2}\text{Prob}[k_1 > k_2 \,|\text{zero sent}] + \tfrac{1}{2}\{[\tfrac{1}{2}\text{Prob}\, k_2 = k_1 \,|\text{one sent}] + \tfrac{1}{2}\text{Prob}\, k_1 = k_2 \,|\text{zero sent}]\} \tag{6}$$

From the symmetry of the transmission method, some of the terms above combine, and the result simplifies. Thus, for the Laguerre counting, (6) becomes

$$PE_L(S, N_0, D) = \sum_{k_1=0}^{\infty} \sum_{k_2=k_1}^{\infty} \gamma_{k_2} P_L(k_1; S, N_0, D) P_L(k_2; 0, N_0, D) \tag{7}$$

where $\gamma_{k_2} = \frac{1}{2}$ for $k_2 = k_1$, and is one otherwise. (The $\frac{1}{2}$ factor accounts for the effect of equal interval counts.) Note that the error probability using Laguerre counting, PE_L, depends explicitly on the count dimension D (time-bandwidth product). If the poisson assumption is applicable, the probabilities in (7) are replaced by those of (5), and we have

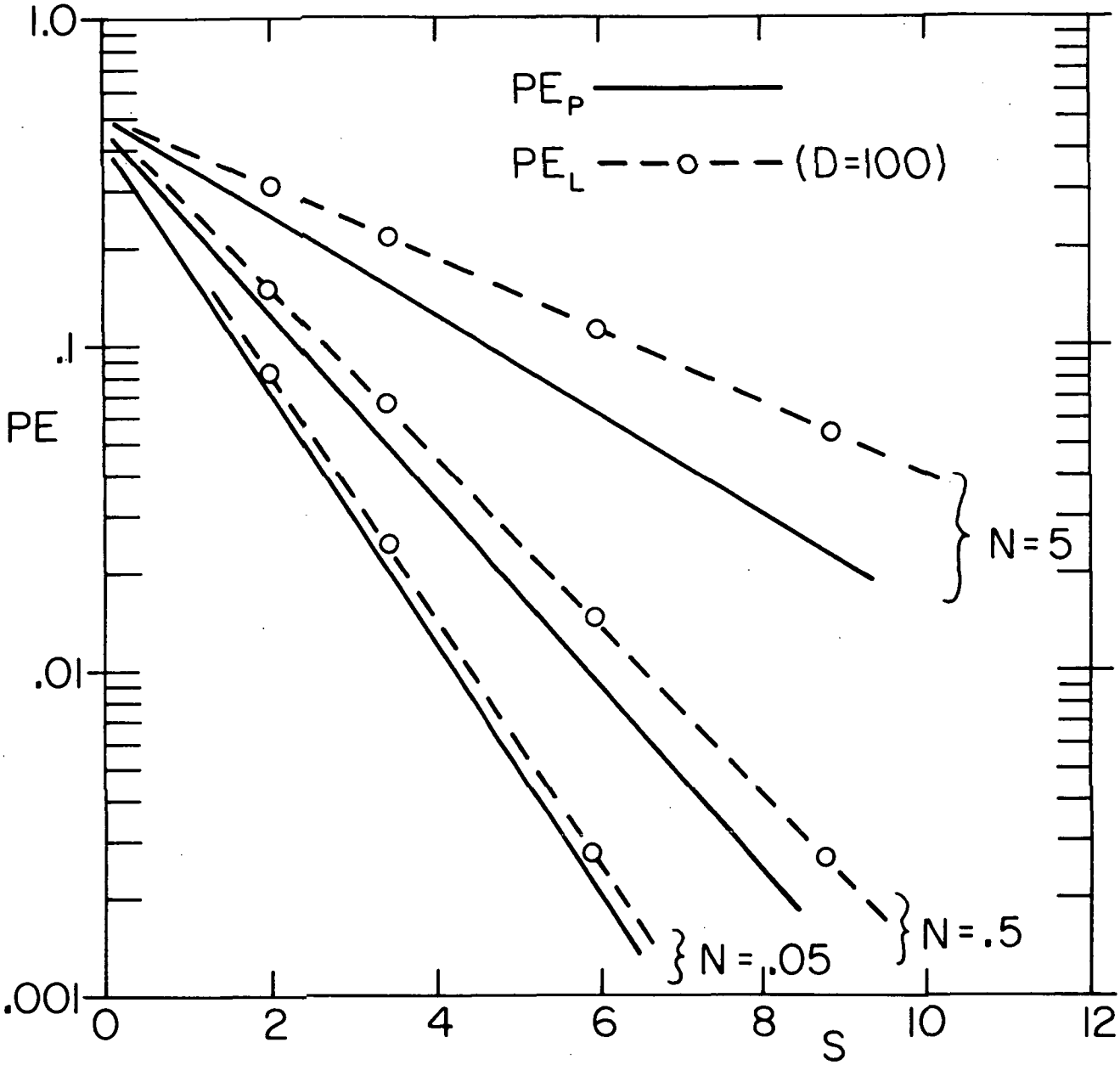

Figure 3.

$$PE_p(S,N) = \sum_{k_1=0}^{\infty} \sum_{k_2=k_1}^{\infty} \gamma_{k_2} P_p(k_1, S+N) P_p(k_2, S+N) \qquad (8)$$

We see that the poisson error probability, PE_p, depends only upon the parameter D through the total noise count $N = DN_0$. The poisson error probability is easier to compute than that using Laguerre counting, and parametric studies of (8) have been extensively published [2,5]. A typical plot of PE_p is shown in Figure 3 as a function of the signal count S. Some PE_L points obtained by computing (7) at the same total noise level are superimposed. Further comparisons of poisson and Laguerre error probabilities, in terms of the parameters involved, are discussed in Reference [6]. The primary conclusion is that at low noise levels ($N \ll 1$), it can be conjectured that $PE_L \approx PE_p$ for moderate ($D \approx 100$) dimensions.

When on-off keying is used, and a threshold test is made at the end of each pulse time T, an error is made whenever the integrator value is on the incorrect side of threshold. If K is the apriori selected threshold count value, then the error probability becomes

$$PE_p(S,N) = \tfrac{1}{2} \sum_{k=0}^{K} \gamma_K P_p(k, S+N) + \tfrac{1}{2} \sum_{k=K}^{\infty} \gamma_k P_p(k, N) \qquad (9)$$

where again $\gamma_K = \frac{1}{2}$ for $k = K$ and is one otherwise. For Laguerre statistics, the probabilities on the right should be replaced by the P_L terms in (2). For poisson counting the sums in (9) are cumulative poisson probabilities, and are well tabulated (e.g. see [9]).

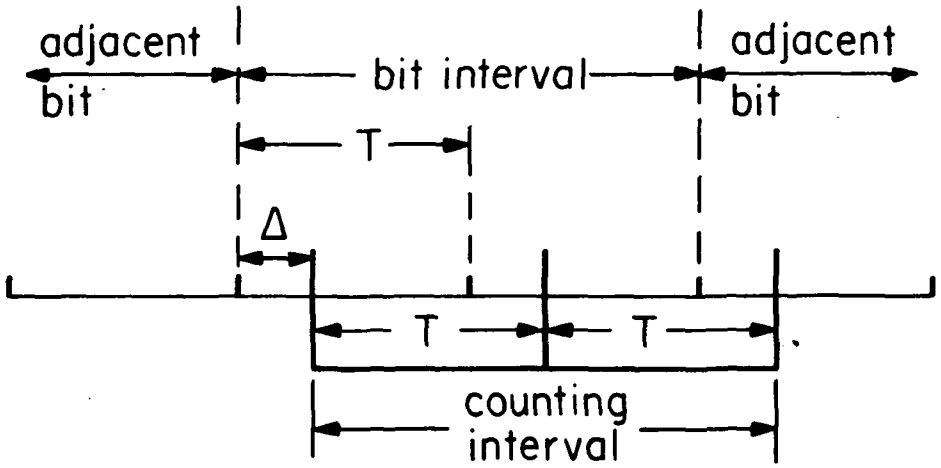
adjacent
bit
bit interval
adjacent
bit
T
Δ
T
T
counting
interval

Figure 4.

Timing Error Effects in PPM

The primary assumption in (8) is that the bit timing is perfect, and the decoder counts photo-electrons exactly over the two T sec intervals that constitute a bit. If a time offset of Δ sec occurs during a bit period, due to timing errors in synchronization lock-up, then the counting occurs over an offset interval. That is, the decoder starts and stops counting over a T sec interval that is displaced by a Δ sec from that containing the bit information, as shown in Figure 4. As a result only a portion of the true signal energy is included in the signal count, while some signal energy may contribute to the count in the adjacent interval, causing intersymbol interference in the form of energy spill-over. The effect of this interference depends upon the form of the adjacent bit; i.e., whether it contains signal energy or not. Assuming a positive timing offset ($0 < \Delta < T$), the various effects on the counting statistics are summarized below, where μ_s is the average signal count rate in (4). If we let $S = \mu_s T$ be the average count over

Transmitted bit	Subsequent bit	Prob $X(0, T)=k_1$	Prob $X(T, 2T)=k_2$
1	0	$P_p[k_1, \mu_s(T-\Delta) + N]$	$P_p[k_2, N]$
1	1	$P_p[k_1, \mu_s(T-\Delta) + N$	$P_p[k_2, N+\mu_s\Delta]$
0	1	$P_p[k_1, \mu_s\Delta + N]$	$P_p[k_2, \mu_s T + N]$
0	0	$P_p[k_1, \mu_s\Delta + N]$	$P_p[k_2, \mu_s(T-\Delta) + N]$

T due to signal energy, and assume equiprobable bits, the error probability for a positive timing error Δ, averaging over all possibilities tabulated above, is then

$$PE_p|_\Delta = \tfrac{1}{2}\sum_{k_1=0}^{\infty}\sum_{k_2=k_1}^{\infty}\gamma_{k_2}P_p[k_1, S(1-\epsilon)+N]P_p[k_2, N+S\epsilon]$$
$$+\tfrac{1}{4}\sum_{k_1=0}^{\infty}\sum_{k_2=k_1}^{\infty}\gamma_{k_2}P_p[k_1, S(1-\epsilon)+N]P_p[k_2, N]$$
$$+\tfrac{1}{4}\sum_{k_2=0}^{\infty}\sum_{k_1=k_2}^{\infty}\gamma_{k_1}P_p[k_1, S\epsilon+N]P_p[S+N] \qquad (10)$$

where $\epsilon = \Delta/T$ is the percentage timing error. The error probability for negative time shifts will be identical to the above, when all possibilities are considered, if we interpret $\epsilon = |\Delta|/T$ when $\Delta < 0$. Note that if each of the double sum terms in (10) is compared to (8) which assumed perfect timing, we can rewrite (10) as

$$PE_p|_\Delta = \tfrac{1}{2}PE_p(S', N') + \tfrac{1}{4}PE_p(S'', N) + \tfrac{1}{4}PE_p(S'', N') \qquad (11)$$

where

$$S' = S(1 - 2\epsilon) \qquad (12a)$$

$$S'' = S(1 - \epsilon) \qquad (12b)$$

$$N' = N + S\epsilon \qquad (12c)$$

Thus, timing errors in PPM can be accounted for by merely reinterpreting the effective signal and noise count per T interval while assuming perfect timing. Note that the timing errors always act to reduce the effective signal energy, while increasing the effective noise, the overall result degrading the error probability. It is important to realize that the fact

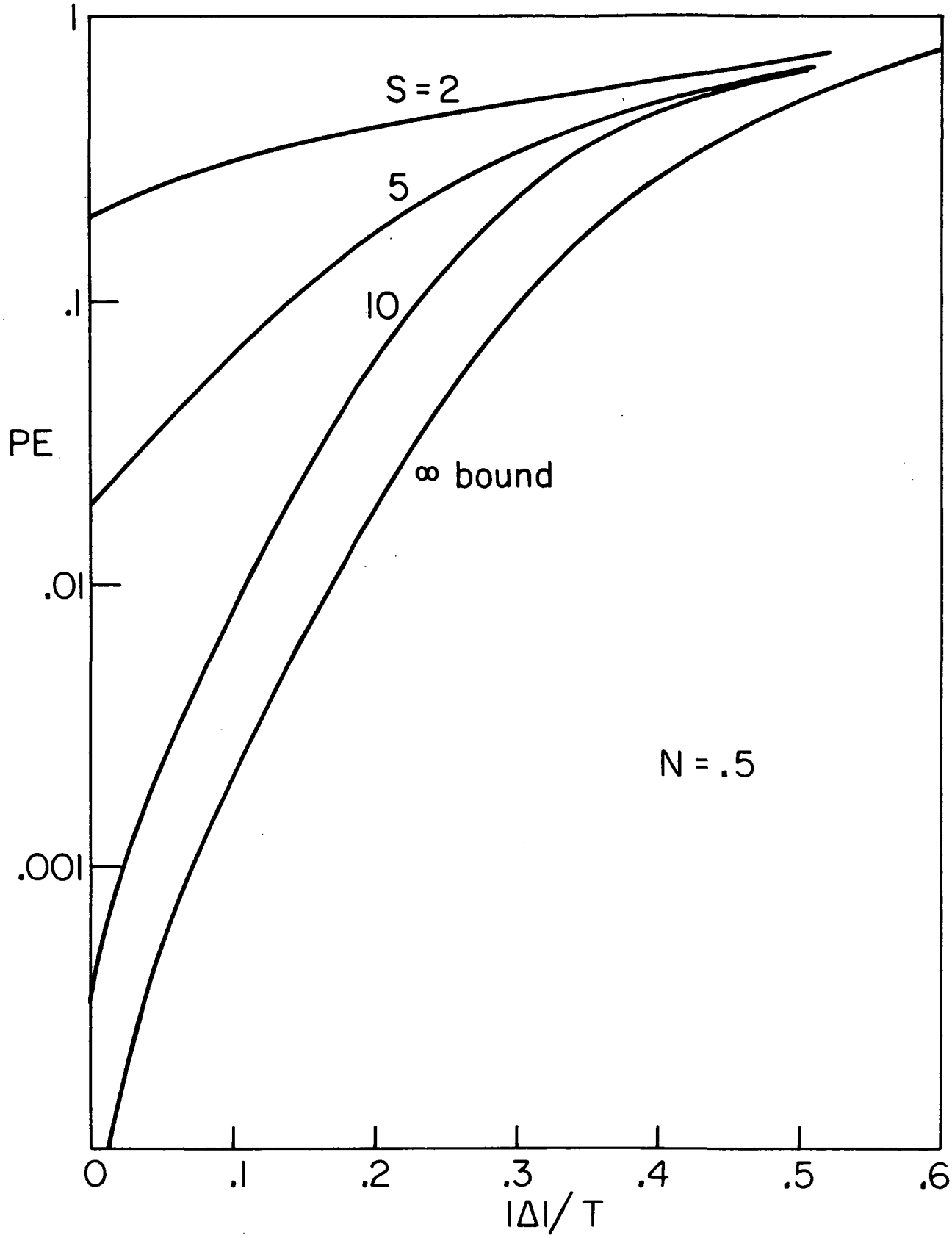

Figure 5.

that the spilled over signal energy appears as effective noise energy is intrinsic in the poisson assumption, and is valid so long as (8) describes the error probability.

A plot of (11), obtained by digital computation, is shown in Figure 5 for positive or negative timing errors. The results show a relatively fast increase in PE (system degradation) as the offset $|\Delta|$ is increased. The system is essentially ruined (PE $\approx .5$) when $\varepsilon \approx .5$ or when $|\Delta| \approx T/2$. (This is the point where the effective signal to noise ratios S'/N' and S''/N', are equal to or less than unity.)

A lower bound to the system performance as $S \to \infty$ is included, obtained by envoking the fact that at low noise levels poisson error probabilities and Laguerre error probabilities with the same total noise are roughly equal, as pointed out before. Since the PE_L monotonically increases with the parameter D, the use of PE_L at D = 0 will serve as a lower bound for error probability. When the signal has count S and the additive noise count is N, (7) with D = 0 is

$$PE_L|_{D=0} = \left(\frac{1}{1+N}\right)^2 \left(\frac{1+2N}{2}\right) \exp[-S/1+N] \sum_{k=0}^{\infty} \left(\frac{1}{1+N}\right)^{2k} L_k\left(\frac{S}{N(1+N)}\right) \tag{13}$$

By applying a Laguerre identity [8, Eq. 8.975] and manipulating algebraically, the above becomes

$$PE_L|_{D=0} = \tfrac{1}{2} \exp\left[\frac{-S}{1+2N}\right] \tag{14}$$

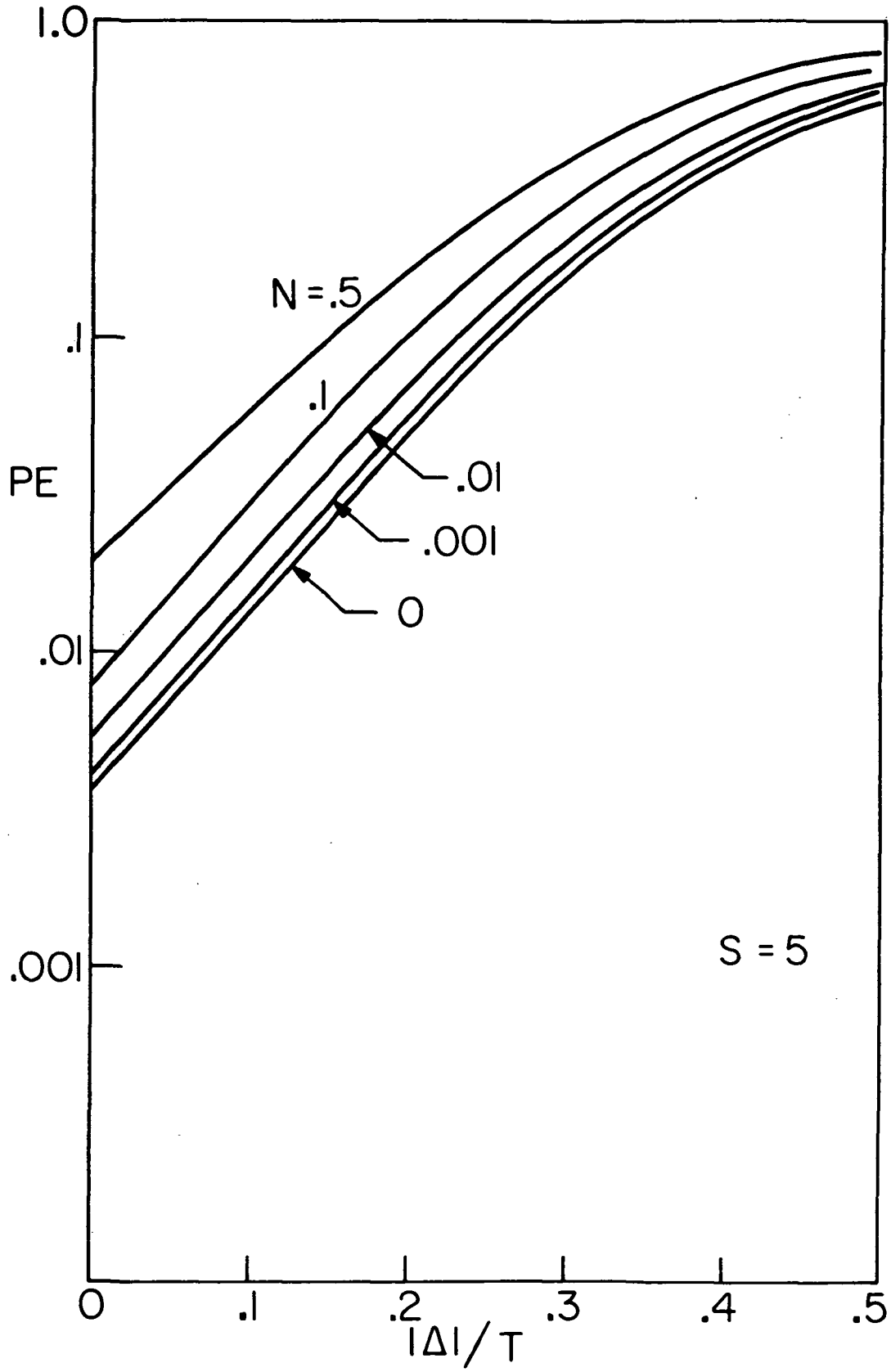

Figure 6.

If we substitute the effective S and N from (12) into (14), and use this as a lower bound for each term in (11), we have

$$PE_p|_{\Delta} \approx PE_L|_{\Delta} \geq PE_L|_{\Delta=0}$$

$$= \tfrac{1}{4} \exp\left[\frac{-S(1 - 2\epsilon)}{1 + 2N + 2\epsilon S}\right] + \frac{1}{8} \exp\left[\frac{-S(1 - \epsilon)}{1 + 2N}\right]$$

$$+ \frac{1}{8} \exp\left[\frac{-S(1 - \epsilon)}{1 + 2N + 2\epsilon S}\right] \qquad (15)$$

Now as $S \to \infty$,

$$\lim_{S\to\infty} PE_p|_{\Delta} \geq \tfrac{1}{4} \exp\left[-\frac{1 - 2\epsilon}{2\epsilon}\right] + \frac{1}{8} \exp\left[-\frac{(1 - \epsilon)}{2\epsilon}\right] \qquad (16)$$

The above lower bound depends only upon ϵ, and is plotted as the $S = \infty$ curve in Figure 5. The result is interesting in that it shows that even as $S \to \infty$, a relatively sharp system degradation can still be expected. This can be attributed again to the fact that timing errors cause a portion of the signal energy to appear as noise energy. Therefore, even though an "infinite" signal energy is available, there is consequently an "infinite" noise energy present, whenever $\epsilon \neq 0$, the overall result not dependent upon S at all, as (16) illustrates.

The behavior of PE_p at different noise counts is shown in Figure 6, for fixed value of S. Again, even with negligible background noise, the system degrades in a similar fashion with increasing timing error.

Timing Error Effects With On-Off Keying

When on-off keyed data bits are transmitted, and threshold tests are used for bit decisions at the decoder, the effect of timing errors can be determined by a procedure similar to the PPM case. The actual bit decisions will be influenced by the adjacent bit (the subsequent bit when $\Delta > 0$, the former bit when $\Delta < 0$), just as in the previous case. If we consider the four possible combinations of transmitted and adjacent bits, and the associated error probability for each, the total error probability when a threshold K is used and an offset Δ occurs, is then

$$PE_p|\Delta = \underbrace{\tfrac{1}{4}\sum_{k=0}^{k} \gamma_k P_p[S+N]}_{11} + \underbrace{\tfrac{1}{4}\sum_{k=K}^{\infty} \gamma_k P_p[N]}_{00}$$

$$+ \underbrace{\tfrac{1}{4}\sum_{k=0}^{k} \gamma_k P_p[S(1-\epsilon) + N]}_{10} + \underbrace{\tfrac{1}{4}\sum_{k=K}^{\infty} \gamma_k P_p[\epsilon S + N]}_{01} \qquad (17)$$

where again $\epsilon = |\Delta|/T$ and S, N are the received signal and noise counts, respectively. The symbols below each sum represent the combination of data bits causing the corresponding error probability, with the left hand bit the transmitted bit and the other adjacent bit. Comparison of (17) with (9) allows us to write

$$PE_p|\Delta = \tfrac{1}{2} PE_p(S, N) + \tfrac{1}{2} PE_p(S', N') \qquad (18)$$

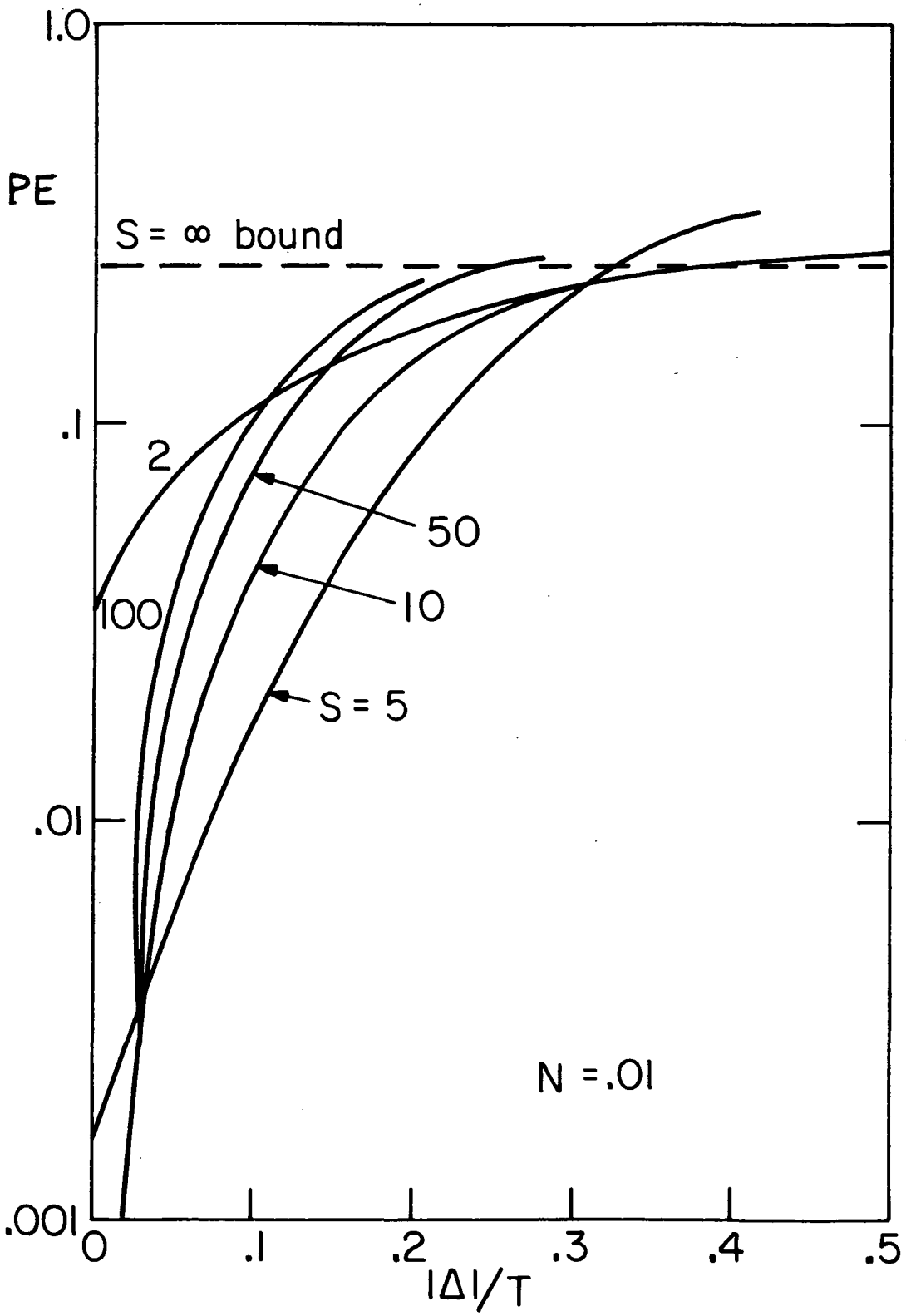

Figure 7.

where the terms on the right are error probabilities with perfect timing, and S' and N' are defined in (12). We again observe that timing error effects can be interpreted as degradations in signal energy and increases in noise energy in a perfectly timed system. Note that timing errors are exhibited only in the second term in (18), and can be attributed to the last two terms in (17), where the adjacent bit is opposite from the true bit. The error probabilities in (18) depend upon the choice of threshold K used for decisioning. For a given design value of S and N, the threshold K that minimizes (9) can be determined by differentiation, and shown to be

$$K = \frac{S}{\log\left(1 + \frac{S}{N}\right)} \tag{19}$$

With this threshold, (18) is plotted in Figure 7 as a function of timing offset for several values of S and N. The curves manifest similar behavior as in PPM, except the degradation is faster, and the curves exhibit crossovers. That is, at small offsets increasing S decreases error probability, but at larger offsets the opposite is true. An examination of the sums in (17) will reveal that for $N \ll 1$, $S \gg 1$ the first three terms tend to zero and the resulting $PE_p \mid \Delta$ is directly attributable to the last term; i.e., the error probability when a zero is sent and the adjacent bit is a one. In the limit as $S \to \infty$, it follows that even though $K \to \infty$ [see Eq. (19)], this latter probability becomes exactly one for any $\epsilon \neq 0$. The overall $PE_p \mid \Delta$ therefore becomes .25, and the result is plotted as the $S = \infty$ curve in Figure 7. The behavior of all these curves can be directly attributed to the fact that optimal on-off keying

requires proper threshold selection, and timing offsets cause changes in effective signal and noise energies and, hence, suboptimal operation. As these effective energies become widely different from the design energies, the resulting system performance is severely degraded.

Random Timing Errors

The timing error that does in fact occur during a bit interval depends upon the synchronization subsystem and its performance in maintaining time lock. This is generally accomplished by tracking a transmitted sync signal with a locally generated sync signal using a feedback tracking loop for error control. The timing error Δ is therefore the tracking error between the received and locally generated sync signals, and in reality should be considered as a random process in t. In typical operation, however, the loop tracking bandwidth is much less than the bit frequency $1/T$, and the assumption of a constant timing error during a given bit interval is essentially valid. The error is however random, and its statistics will depend upon the tracking loop model. When sinusoidal sync signals at the bit frequency $1/T$ are used, and tracking is accomplished by a phase lock loop following photo-detection, the steady state probability density of Δ is given by

$$p(\Delta) = \frac{2\pi}{T} p_{\varphi}\left(\frac{2\pi\Delta}{T}\right) \tag{20}$$

where $p_{\varphi}(\varphi)$ is the density of the loop tracking phase error φ. This latter density has been investigated for a system using a separate optical channel (different optical frequency) for transmitting the sync information [7]. When

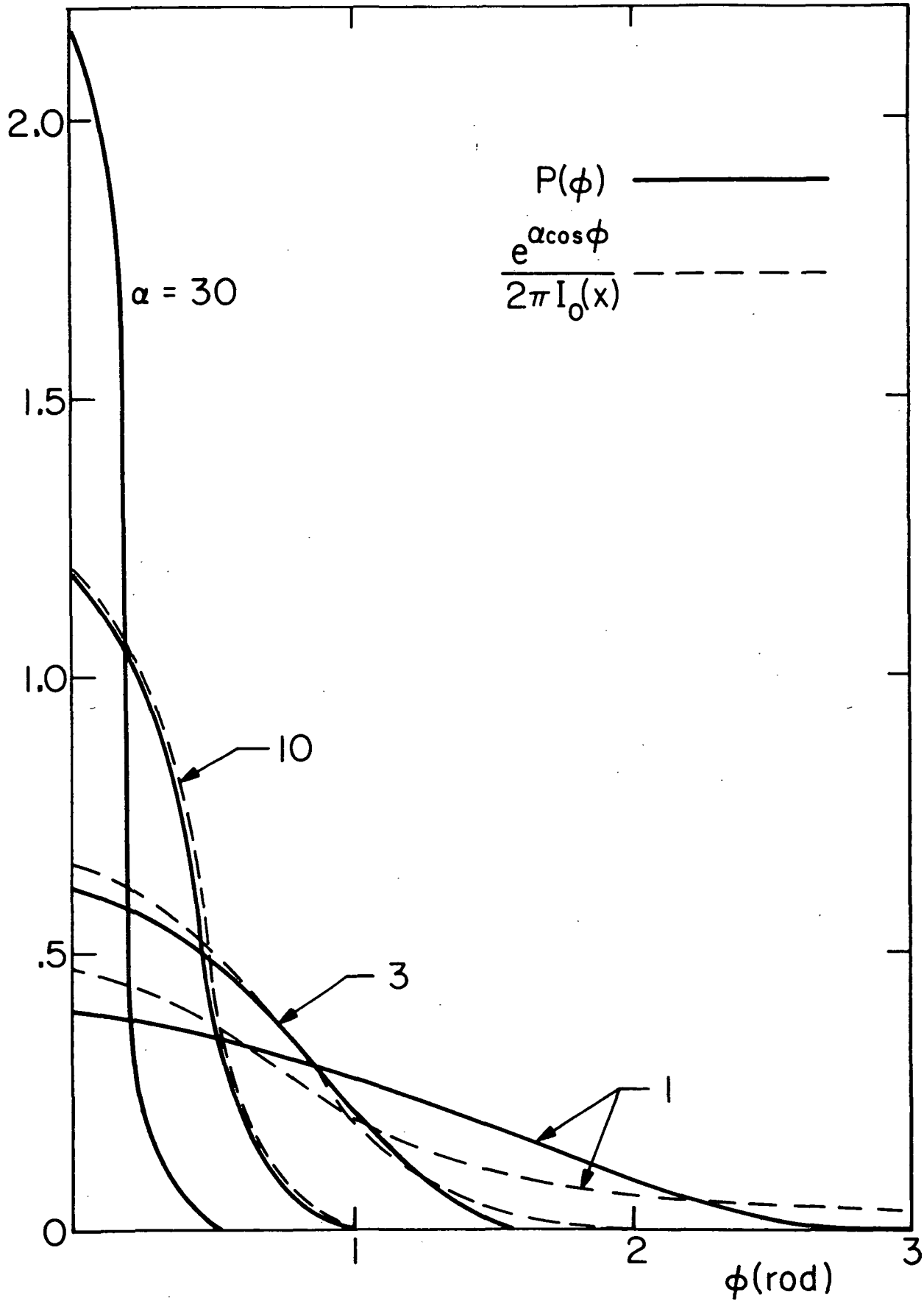
2.0
1.5
1.0
.5
0
1
2
3
ϕ(rod)
$P(\phi)$
$\frac{e^{\alpha\cos\phi}}{2\pi I_0(x)}$
α = 30
10
3
1

Figure 8.

the sync channel is in quantum limited operation (high gain photo-multiplication and negligible background energy) the probability density of the phase error has been computed and the results shown in Figure 8. The phase error density depends only upon the parameter

$$\alpha = \frac{\mu_{sc}}{2B_L} \tag{21}$$

where B_L is the tracking loop bandwidth and μ_{sc} is the average count rate due to the sync signal, the latter directly related to the received power in the sync channel. The parameter α is therefore the average number of sync signal counts occurring in the time period $1/2B_L$. The bandwidth B_L must be selected large enough to allow suitable dynamical tracking of the incoming sync phase shifts (due to doppler, range undertainty, and oscillator phase jitter). For $\alpha \geq 3$, the phase densities are, to a good approximation, given by

$$p_{\varphi}(\varphi) = \frac{\exp[-\alpha \cos \varphi]}{2\pi I_0(\alpha)}, \quad |\varphi| < \pi \tag{22}$$

where $I_0(\alpha)$ is the imaginary Bessel function.

An average timing error probability $\overline{PE}$ can be computed by averaging the $PE|\Delta$ in Figures 5 and 7 over the random timing errors, using the density $p(\Delta)$ obtained from (20). That is,

$$\overline{PE} = \int_{-\infty}^{\infty} [PE|\Delta]\, p(\Delta) d\Delta \tag{23}$$

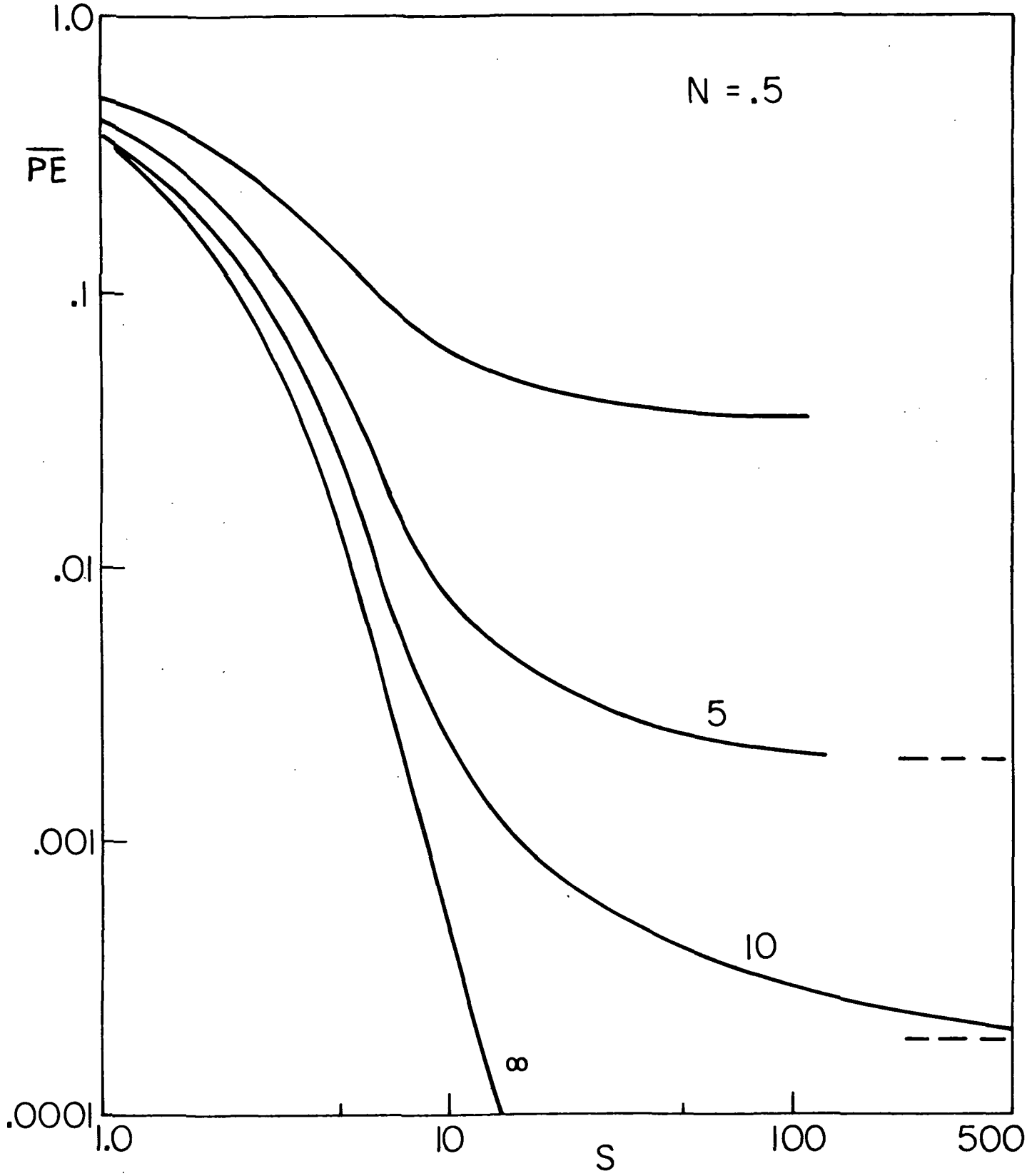

Figure 9.

The integral in (23) was evaluated using a point by point integration of the densities in Figure 8. The results are plotted in Figure 9 for PPM and in Figure 10 for on-off keying, showing $\overline{PE}$ as a function of transmitted data signal count S, for a fixed background noise count N and several signal counts α in the sync channel. The results indicate the average effect of imperfect timing, exhibiting the usual fall off in error probability with increasing signal energy, followed by a flattening (Figure 9) and bottoming (Figure 10) of performance as S is increased. The values of the minimum $\overline{PE}$ depends upon the tracking loop signal count. In PPM the minimum asymptotes plotted in Figure 9 are those obtained by averaging the $S = \infty$ curve in Figure 5 over the densities in Figure 8. In on-off keying $\overline{PE}$ actually begins increasing after achieving a minimum value, even though S continues to increase. (This is due to the fact that the system is more "mismatched" in threshold design at the higher values of S.) This latter fact tends to favor PPM operation over on-off keying when combating imperfectly timed systems. This bottoming of $\overline{PE}$ in both systems is extremely important since it represents a residual, non-reducible error probability that depends only upon the sync system, and cannot be overcome by increasing the bit energy to the data signal. For example, we see from Figure 8 that with $\alpha = 5$ and $N = .5$ we can never achieve an error probability less than 2×10^{-3}, no matter how much pulse energy we transmit. To determine these residual values for other design parameters. The curves for $PE|\Delta$ must be first generated then averaged as in (23).

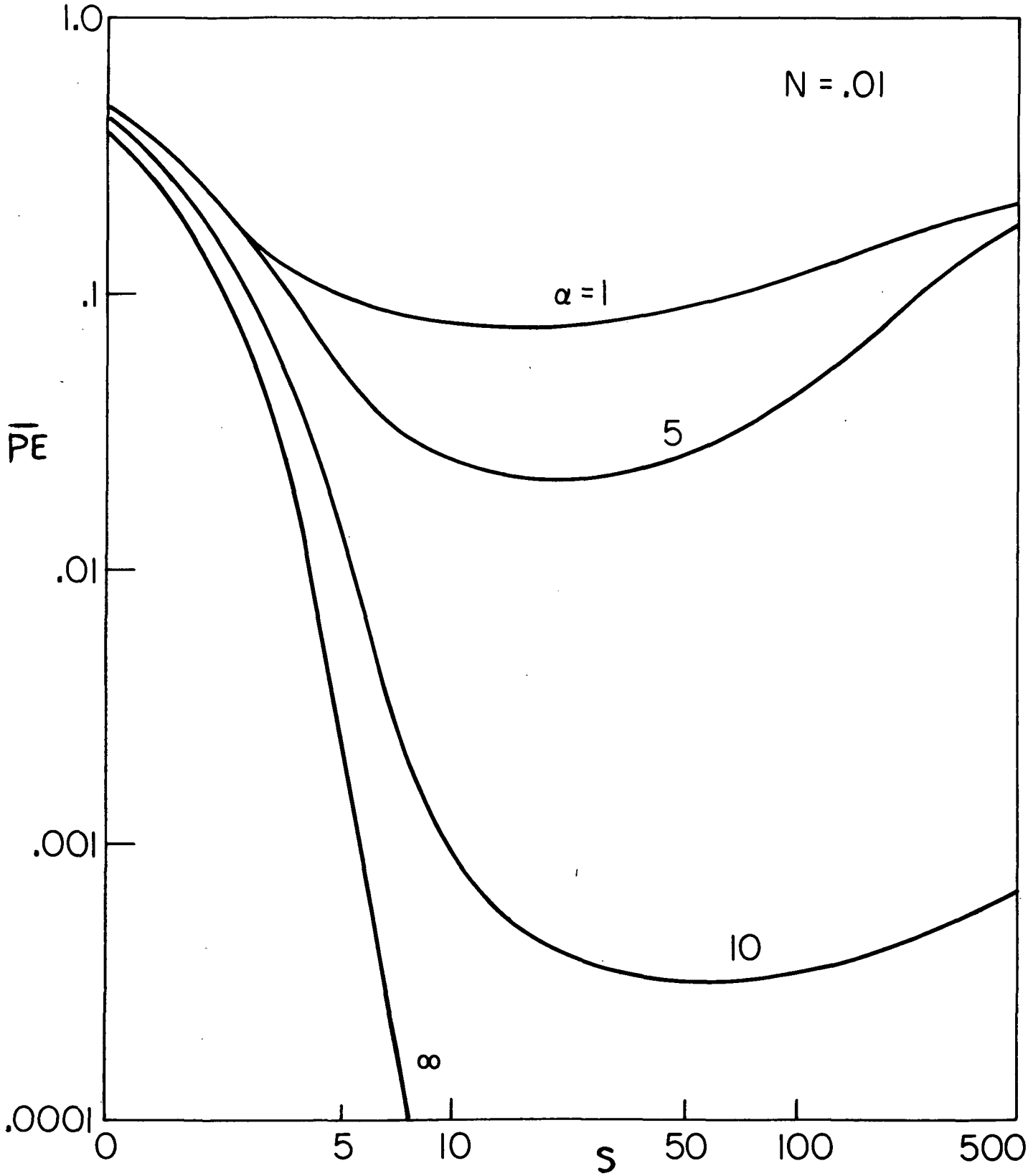

Figure 10.

It may be pointed out that the same residual effect due to imperfect tracking occurs in the additive Gaussian noise channel (microwave system instead of optical) when using phase shift keyed binary transmission. In this latter case, as data signal energy becomes infinite, $PE \to 0$ as long as the tracking error is less than $\pi/2$ radians, and $PE \to 1$ for $\varphi \geq \pi/2$. Thus, the residual error probability is simply the probability that the loop error exceeds $\pi/2$. In Figure 8 we see that as $S \to \infty$ we do not obtain zero PE (except at $\epsilon = 0$), and the residual $\overline{PE}$ tend to be higher than the compatible microwave case. That is, to obtain the same residual $\overline{PE}$, the optical system requires more sync power.

References

[1] IEEE Proceedings, "Optical Communication," Special Issue, October, 1970.

[2] R. Gagliardi, S. Kary, "M-ary Poisson Detection and Optical Communications," IEEE Trans. on Comm. Tech., pp. 208, April, 1969.

[3] S. Karp, E. O'Neill, R. Gagliardi, "Communication Theory for the Free Space Optical Channel," IEEE Proc., October, 1970, p. 1611.

[4] S. Karp, J. Clark, "Photon Counting--A Problem in Classical Noise Theory," IEEE Trans. on Info. Theory, November, 1970.

[5] W. K. Pratt, Laser Communications, (book) Wiley, 1969; Chapter 9.

[6] R. Gagliardi, "Photon Counting and Laguerre Detection," IEEE Trans. on Info. Theory (to be published), January, 1972.

[7] M. Haney, R. Gagliardi, "Optical Synchronization--Phase Locking with Shot Noise Processes," USCEE Report 396, August, 1970.

[8] I. Gradsteyn, I. Ryzhik, Tables of Integrals, Series, and Products, (book) Academic Press, 1965.

[9] M. Abromowitz and I. Stegun, Handbook of Mathematical Functions, (book) National Bureau of Standards, June, 1964, Table 26-7.


USG
Engineering